Cis-regulation of gene expression between sexes and life stages in *Rumex hastatulus*

Meng Yuan[1,†], Bianca M. Sacchi[1], Baharul I. Choudhury[1,2], Spencer C. H. Barrett[1], John R. Stinchcombe[1,*], Stephen I. Wright[1,*]

[1]Department of Ecology and Evolutionary Biology, University of Toronto, Toronto, ON, CA

[2]Department of Biology, Queen's University, Kingston, ON, Canada

*These authors made equal contributions.

†Corresponding author: E-mail: my.yuan@mail.utoronto.ca

Abstract

The potential for conflict between sexes and life stages while sharing predominantly the same genome has important evolutionary consequences. In dioecious flowering plants, genes beneficial for the haploid pollen stage may reduce the fitness of diploid offspring of both males and females. Such antagonistic pleiotropy between sexes and life stages can in some cases maintain genetic variation. However, we still lack understanding of the extent of shared genetic architecture for gene expression between the sexes or life stages in plants, a key component for predicting the scope for conflict. We performed expression quantitative trait loci (eQTL) mapping to test if standing variation affects sexes and life stages differently using a population sample of the dioecious outcrossing plant *Rumex hastatulus*. We compared effect sizes and allele frequencies of *cis*-eQTLs in male and female leaf tissues and pollen, and tested for genotype-by-sex interactions for gene expression. We found stronger shared genetic architecture between sexes than between the life stages. In addition, comparisons of the site frequency spectra for *cis*-eQTLs to a null distribution found no evidence for a genome-wide pattern consistent with purifying selection. Our results suggest that any conflict over optimal gene expression between pollen and leaves may be easily resolved due to their distinct genetic architectures, whereas there is more scope for conflict between the sexes in gene expression for leaves. Our study highlights the use of eQTL mapping to infer the scope of shared genetic architecture and for investigating the evolution of conflict between sexes and life stages in dioecious species.

Keywords: *cis*-regulatory variation, eQTL, selective pressure, antagonistic pleiotropy

Author Summary

Conflict may arise when different sexes or life stages have contrasting 'evolutionary interests'. The degree of shared genetic basis between sexes or life stages in a phenotypic trait such as gene expression can indicate whether there is the scope for ongoing conflict. We identified cis-regulatory variation using expression quantitative loci (eQTL) mapping in leaf and pollen tissues of a dioecious plant, and tested the scope of conflict between sexes and life stages. We found more shared eQTLs and stronger positive correlation in their effects on expression between sexes than life stages, suggesting more shared genetic basis and higher potential for ongoing conflict between sexes than life stages. In addition, we tested selective pressures on cis-regulatory variation using allele frequencies and found similar patterns of selective pressures on eQTLs between sexes and life stages with an overabundance of rare alleles. By comparing to a null distribution, the excessive rare alleles in eQTLs did not suggest a genome-wide signal of purifying selection.

Introduction

Evolutionary conflict may arise when different sexes or life stages of an organism have different fitness optima while sharing a common genome [1–4]. For example, sexual conflict occurs when males and females have different fitness optima involving reproduction and this can drive sexual dimorphism in phenotypic traits (reviewed in [2]). In plants, the diploid and haploid life stages are distinct in their morphology, development, and genetics despite sharing extensive overlap in gene expression, creating potential for genetic trade-offs [3,5]. Both sexual and life-stage conflict have been suggested to generate balancing selection and stable genetic variation under some conditions [6,7]. However, we lack comprehensive understanding of the traits and genetic architecture underlying the conflict between sexes or life stages. Here, we use expression quantitative trait locus (eQTL) mapping to identify genome-wide *cis*-regulatory variation and investigate the extent of shared genetic architecture between sexes and life stages and the scope for sexual and life-stage conflict in a dioecious plant species.

Current empirical examples of life-stage conflict often involve both sexes (i.e., a conflict both between the sexes and life stages). For example, alleles beneficial for haploid gametophytic competition were shown to reduce the fitness of female diploid offspring in the hermaphroditic annuals *Clarkia* [8] and *Collinsia* [9]. In *C. heterophylla*, pollen donors that induce early stigma

63 receptivity, thus increasing paternity, reduced seed set [9–11]. However, sexual selection and
64 sexual conflict in sessile plants involving one or both life stages still remain understudied
65 compared to the extensive evidence from numerous animal species [12,13]. The diverse
66 reproductive systems in plants provide a unique opportunity to study sexual conflict, from
67 conflict between female and male function in hermaphrodites [14] to sexual dimorphisms in
68 dioecious species and the resolution of intralocus sexual conflict [15]. Additionally, because of
69 the considerable scope for both sexual and life-stage conflict in plants, whether there is more
70 scope for one type of conflict than the other, or whether one type of conflict is more resolved
71 than the other, remains unanswered.
72
73 The scope for conflict will depend on the degree of shared genetic architecture between sexes or
74 life stages. For example, high genetic correlation in a trait between sexes may constrain the
75 responses to antagonistic selection and the evolution of sexual dimorphism [16–18]. Gene
76 expression is an important molecular trait underlying phenotypic variation, and sexual
77 dimorphism in gene expression is likely a key driver of the phenotypic divergence between sexes
78 [19]. Genetic covariances between sexes have been inferred through gene expression studies in
79 *Drosophila melanogaster* suggesting considerable scope for ongoing conflict [20–22]. Similarly,
80 whether genetic correlations in traits across life stages commonly constrain their independent
81 evolution under opposing selection is an important unresolved question.
82
83 Expression quantitative trait loci (eQTL) mapping is useful for identifying loci underlying
84 regulatory variation and testing the genome-wide importance of selection [23–25]. *Cis*-
85 regulatory variation has a relatively large effect on gene expression, making it easier to map *cis*-
86 eQTLs in association studies [26,27]. Selective pressure on eQTLs can be inferred from their
87 distribution of allele frequencies; an excess of rare alleles will indicate purifying selection that
88 removes deleterious mutations, whereas an excess of common alleles indicates balancing
89 selection maintaining genetic variation. In the leaf tissues of *Capsella grandiflora*, trans-eQTLs
90 were found to be under stronger purifying selection than *cis*-eQTLs [25,28]. In contrast, in floral
91 tissues of *Mimulus guttatus*, trans-eQTLs showed signatures of purifying selection whereas *cis*-
92 eQTLs showed signatures of balancing selection based on their allele frequencies [29]. These
93 studies from two species suggest eQTLs can act differently in different contexts, suggesting the
94 possibility of differential selection on genes expressed in different sexes or life stages.

95

96 In addition to testing the genome-wide importance of purifying versus balancing selection on
97 regulatory variation, eQTLs can be used to test whether standing variation affects sexes or life
98 stages concordantly. A study on *cis*-eQTLs in 44 human tissues between sexes found that despite
99 a moderate number of genes showing sex-biased expression, *cis*-eQTLs showing Genotype ×
100 Sex interaction were much rarer [30]. In *Drosophila melanogaster* somatic tissues, more *cis*-
101 regulatory variation was found in unbiased and moderately biased than strongly biased genes
102 between sexes. This finding suggested that the former genes experience potential ongoing sexual
103 conflict in regulatory variation [31,32]. Despite the importance of understanding the scope of
104 genome-wide conflict, we still lack tests on the extent of shared genetic architecture between
105 sexes or life stages, especially in dioecious plant species where both types of conflict in one
106 system can be compared.
107
108 In this study, we tested *cis*-regulation in gene expression through *cis*-eQTL mapping in the
109 dioecious, wind-pollinated and obligately outcrossing annual *Rumex hastatulus* (Polygonaceae).
110 Several observations in *R. hastatulus* indicate the potential for antagonism between sex and life
111 stages, especially during pollen competition. Female biased sex ratios are observed in *R.*
112 *hastatulus*, likely due to greater competitive ability of female-determining pollen following Y-
113 degeneration [33,34], and gametophytic selection is suggested to play a role in sex chromosome
114 evolution in this species [35–37]. Sexual dimorphism related to wind pollination in both
115 vegetative and reproductive traits occur in *R. hastatulus*, e.g., males are taller and produce more
116 inflorescences during peak flowering, presumably to maximize access to female flowers [31].
117 The potential conflict between sexes and life stages in *R. hastatulus* makes it a promising
118 experimental system to test the direction of selection on gene expression between sexes and life
119 stages and also to compare the scopes for sexual versus life-stage conflict.
120
121 We tested differential gene expression between sexes and life stages, and mapped *cis*-eQTLs
122 separately in leaf and pollen tissues to compare their effect sizes and allele frequencies. We
123 found significantly fewer differentially expressed genes between sexes than between life stages,
124 and most of the highly sex-biased genes were on the sex chromosomes. There was a greater
125 overlap in eGenes and eQTLs between sexes than life stages. Effect sizes of eQTLs were
126 positively correlated between sexes and life stages, with a much stronger correlation between

127 sexes, indicating more shared genetic architecture between sexes. Consistent with this result, we
128 found limited Genotype × Sex interaction in gene expression. There were a large number of
129 eQTLs driving the divergent expression between life stages. Lastly, we found similar allele
130 frequency distributions of eQTLs among tissues, suggesting similar selective pressures in eQTLs
131 between sexes and life stages but no excess of rare alleles among eQTLs in any tissues when
132 compared to a null distribution.
133
134 **Results**
135 *Differential expression between sexes and life stages*
136 Using leaf tissue to represent the diploid stage and pollen the haploid stage, we performed
137 differential gene expression analyses to identify sex-biased genes in leaves and life stage-biased
138 genes between pollen and male leaf tissues (S2 Table). Among the 37,659 annotated genes
139 across the genome, we first filtered for genes with evidence of expression in at least one of the
140 two tissues being compared, resulting in 19,494 genes in the between-sex comparison and 21,337
141 genes in the between-life-stage comparison. In a principal component analysis (PCA) of RNA
142 read counts, pollen and male leaf samples were separated by PC1 that explained 99% variance
143 both before and after excluding sex-specific regions on sex chromosomes (S1 Fig). Male and
144 female leaf samples were separated by PC1 which explained 52% of the variance when sex-
145 specific regions were included but were not separated based on autosomal and pseudoautosomal
146 (PAR) genes (S1 Fig). Consistent with the PCA results, there were over 10-fold more
147 differentially expressed (DE) genes between life stages (16,649) than between sexes (1,496)
148 (adjusted $p < 0.05$, fold change > 2, S2 Table).
149
150 We tested for enrichment of DE genes on sex chromosomes and the overlap between sex-biased
151 and life stage-biased genes. Sex-biased genes were highly enriched on sex chromosomes (S2
152 Table), with 378 out of 405 female-biased genes on the X-specific regions and 1,026 out of 1,091
153 male-biased genes on the Y-specific regions (adjusted $p < 0.05$, fold change > 2). Among 6,702
154 pollen-biased genes, there was an excess of over-expression of these genes in male leaf
155 compared to female leaf (30 on autosomes and PAR, 1 on X, 269 on Y) tissue compared to
156 female-biased genes (7 on autosomes and PAR, 63 on X, 3 on Y) (Fisher's exact test, $p =$
157 0.0028). Although it was a relatively small subset of pollen-based genes, the larger overlap
158 between male leaf-biased and pollen-biased genes was mostly driven by the Y-specific regions.

159 This finding implies that selection for higher gametophytic expression in pollen could have
160 pleiotropic effects on expression in male leaves (and *vice versa*), which could lead to
161 antagonistic or synergistic pleiotropy for gene expression depending on the direction of selection
162 on expression between life stages.
163
164 A previous study in two *Rumex* species found an enrichment of pollen-biased genes on sex
165 chromosomes relative to autosomes, suggesting a role of male gametophytic selection in Y
166 chromosome evolution [37]. With a new PacBio genome assembly containing X and Y phased
167 assemblies [38], we attempted to replicate these results with our gene expression data in *R.*
168 *hastatulus*. In accord with the earlier results, we found a significant enrichment of pollen-biased
169 genes on the Y chromosome compared to the autosomes or the X chromosome (S2 Fig, Fisher's
170 exact test, $p = 0.007$ for autosomes, $p = 0.001$ for X) specifically for highly pollen-biased genes
171 (fold change > 4). Among moderately pollen-biased genes (fold change > 2), we found a
172 significant enrichment of pollen-biased genes on the Y chromosome only when compared to the
173 X chromosome (S2 Fig, Fisher's exact test, $p = 0.031$ for X, $p > 0.1$ for autosomes).
174
175 *eQTLs between sexes and life stages*
176 To test whether *cis*-eQTLs affect expression concordantly between sexes or life stages, we
177 performed *cis*-eQTL mapping separately in male leaf, female leaf and pollen. We obtained
178 4,509,904 and 3,288,995 SNPs on autosomes from 74 female and 69 male leaf DNA samples,
179 respectively, after removing variants with low minor allele frequency or strong Hardy–Weinberg
180 deviations. Based on Tracy-Widom tests, we found 5 and 6 significant PCs for female and male
181 samples explaining 6.53% and 7.7% of genetic variation, respectively (TW statistic ≥ 1.068, $p \leq$
182 0.0441 for females; TW statistic ≥ 2.288, $p \leq 0.00634$ for males); we included the significant
183 PCs as covariates in eQTL mapping.
184
185 We identified *cis*-eQTLs and genes whose expression was influenced by eQTLs ("eGenes") in
186 male leaf, female leaf and pollen (Table 1, S3 Fig). We found more shared eGenes and eQTLs
187 between male and female leaf than between male leaf and pollen (**Fig 1a-b**). The number of
188 eQTLs per eGene ranged from 1 to 126 in pollen, 1 to 170 in male leaf, and 1 to 268 in female
189 leaf, with a median of 2 eQTLs per eGene in both male leaf and pollen, and 3 in female leaf. We
190 found eQTLs were located closer to their associated eGenes than the nearby SNPs tested in all

191 tissues (median distance to the transcription start site: 7718 - 7893 bp for eQTLs vs. 8982 - 9254
192 bp for nearby SNPs). There were similar numbers of eQTLs upstream and downstream of the
193 transcription start site (S4 Fig). We found a strong negative correlation between minor allele
194 frequencies and effect sizes of eQTLs in all tissues when selecting the most significant eQTL
195 (top eQTL) per eGene (Spearman correlation, r = -0.60 ~ -0.65, $p < 10^{-16}$) and when selecting a
196 random eQTL per eGene (r = -0.71 ~ -0.75, $p < 10^{-16}$) (S5 Fig). There was a weak but significant
197 negative correlation between effect sizes of eQTLs and their distance to the transcription start
198 site in all tissues when selecting the top eQTL (Spearman correlation, r = -0.04 ~ -0.09, $p <$
199 0.041) and also when selecting a random eQTL (r = -0.06 ~ -0.11, $p < 0.001$).
200
201 **Table 1. eQTL mapping in male leaf, female leaf and pollen on autosomes. FDR = 0.1.**

	Number of samples	Number of phenotypes tested	Number of nearby SNPs tested	Number of eGenes	Number of eQTLs	Number of eQTLs affecting multiple genes	Number of secondary eQTLs
Male leaf	69	14,777	1,272,993	2,421	16,674	486	367
Female leaf	74	14,564	1,687,298	3,442	34,238	905	722
Pollen	69	13,785	1,182,102	1,475	9,456	201	159

202

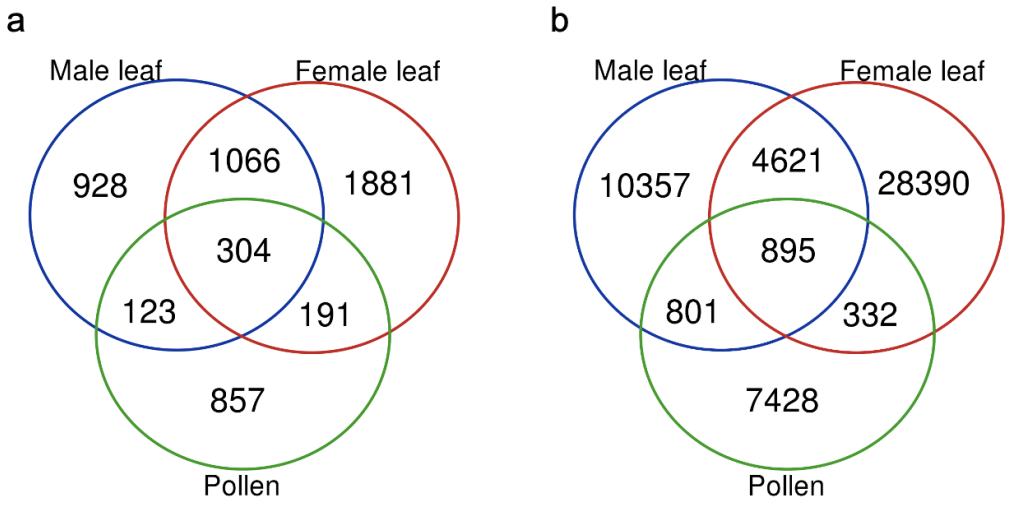

203
204 **Fig 1. Venn diagrams of eGenes (a) and eQTLs (b) between sexes and life stages on**
205 **autosomes of *Rumex hastatulus*.** FDR = 0.1.
206

207 In addition to the primary eQTLs in each tissue, for each eGene we examined the independence
208 of its eQTLs and identified secondary eQTLs (Table 1, see Methods). Secondary eQTLs were
209 considered as conditionally independent after accounting for the effect of the primary eQTL of
210 each eGene. We found primary eQTLs were significantly closer to the transcription start site
211 than secondary eQTLs in female leaf and male leaf tissue (*t*-test, $p = 0.02$, 0.009, 0.32 for female
212 leaf, male leaf, pollen, respectively). There were 40 - 43% of secondary eQTLs that had opposite
213 effects compared to the primary eQTL of the eGene, consisting of 0.7 - 0.9 % of all eQTLs in
214 each tissue (158 for male leaf, 291 for female leaf, 63 for pollen). The minor allele frequencies of
215 primary and secondary eQTLs were not significantly different (Mann-Whitney *U*-test, $p = 0.12$,
216 0.37, 0.22 for male leaf, female leaf, pollen, respectively).
217
218 We performed gene ontology enrichment of eGenes in each tissue and examined whether they
219 showed transcriptional or protein biosynthesis functions. Different tissues showed different
220 patterns of functional enrichment (S3 Table). For example, female leaf tissue showed enrichment
221 for protein metabolic process (GO:0019538) whereas pollen showed enrichment for mRNA
222 metabolic process (GO:0016071) and negative regulation of gene expression (GO:0010629).
223 Additionally, protein deubiquitination (GO:0016579) was enriched in both male leaf and pollen,
224 and regulation of RNA metabolic process (GO:0051252) was enriched in female leaf and pollen.
225
226 *Shared genetic basis between sexes and life stages*
227 To investigate the extent of shared genetic architecture in expression between sexes and life
228 stages, we first estimated the correlation in expression level across genes between sexes and life
229 stages. For comparing sexes, we estimated the correlation in expression between male and
230 female siblings, which is a phenotypic approximation of the genetic correlation between sexes
231 (r_{mf}). For comparing life stages, this represents the phenotypic correlation between traits, which
232 reflects both environmental and genetic variances. We found expression levels were more
233 positively correlated between sexes than life stages based on all genes and eGenes (**Fig 2a-b**,
234 Mann-Whitney *U*-test, $p < 10^{-16}$ in both comparisons). Even though correlations between life
235 stages involve the same individual (as opposed to siblings of the opposite sex, for comparing the
236 sexes), the stronger correlation in expression between sexes, suggests potentially more shared
237 genetic basis between sexes than life stages.

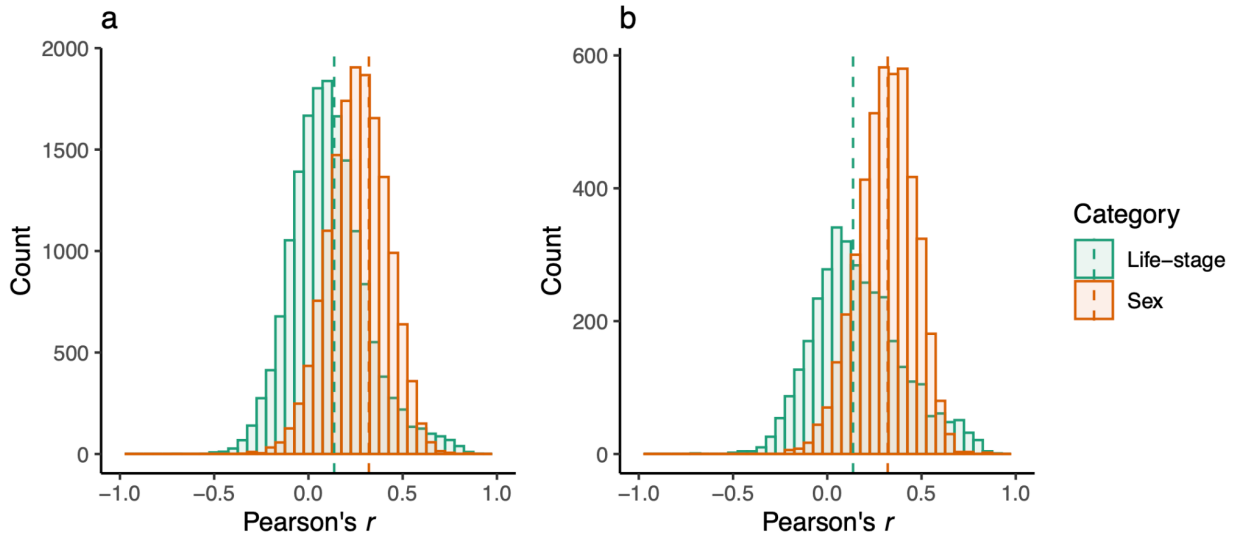

Fig 2. Distribution of Pearson correlation coefficients in gene expression between sexes or life stages in all genes (a) and in eGenes (b) in *Rumex hastatulus*. The dashed line represents the median of each group: 0.093 (Sex) 0.27 (Life-stage) in a, and 0.14 (Sex) 0.32 (Life-stage) in b. Numbers of genes: 14992 (Sex) and 16411 (Life-stage) in a, 4493 (Sex) and 3469 (Life-stage) in b.

Next, we tested whether *cis*-regulatory variation had concordant or discordant effects in gene expression between sexes and life stages. We filtered for nearby SNPs tested in both sexes or life stages that were the top eQTL for the eGene in at least one sex or life stage, resulting in 2,420 eQTLs in the sex comparison and 3,077 eQTLs in the life-stage comparison. The majority of eQTLs showed concordant effects between both sexes and life stages, with their effect sizes positively correlated (**Fig 3a-b**). The correlation of eQTL effect sizes was much stronger between sexes (Spearman correlation, $r = 0.72$, $p < 10^{-16}$) than between life stages ($r = 0.35$, $p < 10^{-16}$), suggesting a stronger shared genetic architecture between sexes (**Fig 3a-b**), as would be predicted from the phenotypic correlations in **Fig 2a-b**. There were 170 eQTLs with opposite effects between sexes, all of which were the top eQTL in one sex but not an eQTL in the other sex (light orange and light purple dots in **Fig 3a**). There were 974 eQTLs with opposite effects between life stages, 19 of which were eQTLs in both life stages (S6 Fig). Functional enrichment of eGenes with eQTLs showing opposite effects between sexes or life stages showed an enrichment in processes relevant to transcription including negative regulation of gene expression (GO:0010629) and regulation of DNA-templated transcription (GO:0006355), and

260 processes post transcription including regulation of RNA and protein metabolic processes
261 (GO:0051252, GO:0051246) (S4 Table).

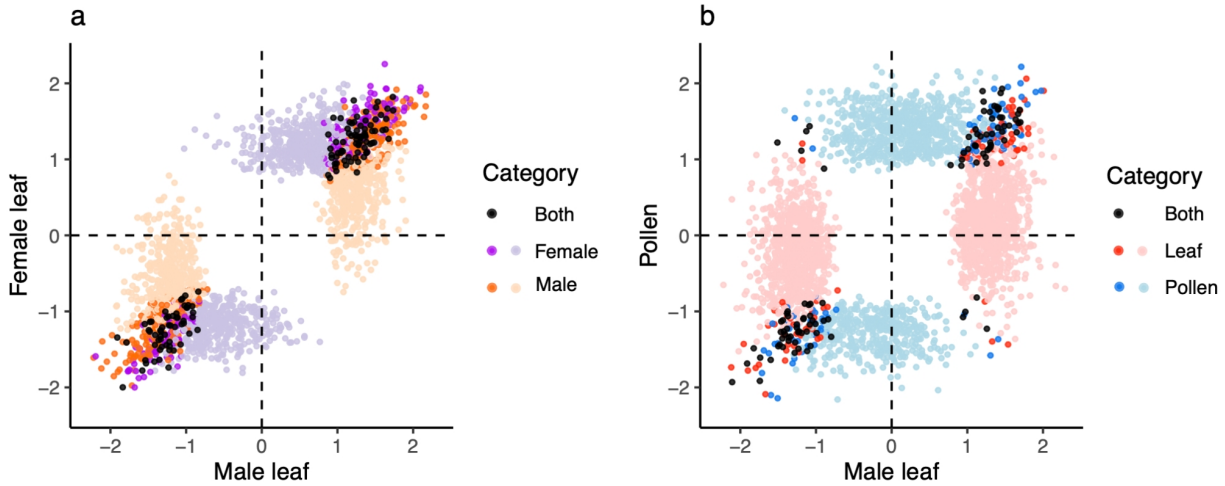

262

263 **Fig 3. Correlation of effect sizes of autosomal SNPs tested between sexes (a) and life stages**
264 **(b) in *Rumex hastatulus*.** Black: top eQTL of the eGene in both sexes or life stages; darker
265 colors: top eQTL in the labelled sex/life stage, significant but not the top eQTL in the other
266 sex/life stage; lighter colors: top eQTL in the labelled sex/life stage but not significant in the
267 other sex/life stage. Spearman correlation coefficients: 0.72 (a), 0.35 (b).

268

269 *Genotype × Sex interaction*

270 We obtained 3,684,937 SNPs on autosomes from 143 leaf DNA samples to test for Genotype ×
271 Sex interactions in *cis*-regulatory variation. We found one significant PC in all leaf samples
272 combined that explained 2% of genetic variation (TW statistic = 1.328, $p = 0.0302$) and we
273 included it as a covariate in eQTL mapping. We tested 14,587 genes and 1,083,706 nearby SNPs
274 for the effect of Genotype, Sex, and Genotype × Sex interaction on expression. After the
275 correction for multiple testing [39], we found 5 eQTLs showing significant Genotype × Sex
276 interaction (adjusted $p < 0.1$, see Methods), all of which changed expression of their eGene in the
277 same direction but with different magnitudes (S7 Fig). The small number of eQTLs showing
278 Genotype × Sex is consistent with the previous result that eQTLs showed strongly correlated
279 effects between sexes (**Fig 3a**).

280

281 *eQTLs for expression differences between life stages*

282 We tested 16,218 genes and 1,404,801 nearby SNPs for *cis*-eQTLs affecting the degree of
283 expression differences between life stages. Specifically, we calculated the effect sizes of the
284 minor allele of each SNP on the differences in expression levels between male leaf tissue and
285 pollen. We found 9,873 eQTLs affecting the expression differences between life stages in 1,564
286 genes. There were more eQTLs in which the minor allele increased expression differences
287 (6,173) than reduced them (3,700), suggesting new mutations (typically represented by the minor
288 alleles) more often drive the divergence in expression between life stages than constrain it. We
289 found 1,464 of 1,564 genes whose expression differences between life stages were affected by
290 eQTLs were significant DE genes between pollen and male leaf tissue (adjust $p < 0.05$, no fold
291 change cutoff). Compared to all DE genes, these 1,464 genes were enriched for high expression
292 bias (fold change > 8) and underrepresented for low expression bias (fold change < 2) (Chi-
293 squared test, $p < 10^{-10}$; Pearson residuals = 3.37, -4.95, respectively), likely reflecting that highly
294 pollen-biased genes have more pollen-specific regulatory functions. We found rRNA processing
295 (GO:0006364) and regulation of RNA metabolic processes (GO:0051252) were enriched in
296 genes with eQTLs affecting life-stage expression differences (S5 Table). Lastly, we identified
297 141 conditionally independent eQTLs affecting life-stage expression differences, 54 of which
298 had opposite effects compared to the primary eQTL of the same gene.
299
300 We examined whether eQTLs for expression differences between life stages were also identified
301 as eQTLs in male leaf tissue or pollen separately. We mapped eQTLs in male leaf and pollen
302 testing the effects of minor alleles on expression. There were 1,051 genes whose expression
303 differences were significantly affected by *cis*-regulatory variation and were also tested for eQTLs
304 in both male leaf and pollen individually. Of the 5,946 eQTLs associated with expression
305 differences in these 1,051 genes, 5,027 were also identified as eQTLs in at least one life stage,
306 while the remaining did not pass the multiple testing filters to be eQTLs. There were 767 eQTLs
307 that significantly affected leaf expression, pollen expression, and the differences between them,
308 735 of which affected leaf and pollen expression in the same direction, consistent with the
309 concordance in eQTL effect sizes shown in **Fig 3b**.
310
311 *Selective pressure on eQTLs*
312 We examined the distribution of minor allele frequencies (MAF) of eQTLs to test if selective
313 pressure differs for eQTLs between sex or life stages. An excess of low-frequency variants

314 indicate purifying selection, whereas an excess of intermediate-frequency variants indicate
315 balancing selection [40]. We kept one eQTL per eGene to have a set of independent eQTLs for
316 MAF comparisons and repeated the analyses when keeping the top eQTL and a random eQTL.
317 In all tissues, there was an excess of rare alleles (**Fig 4a-f**). The median MAFs between tissues
318 were similar, with the highest median MAF in female leaf and lowest median MAF in male leaf
319 using both methods of eQTL selection. The differences in mean MAFs between tissues were
320 marginally significant between male and female leaf in top and random eQTLs (Mann-Whitney
321 *U*-test, $p = 0.041$, 0.049, respectively) and between female leaf and pollen in top eQTLs (Mann-
322 Whitney *U*-test, $p = 0.049$).

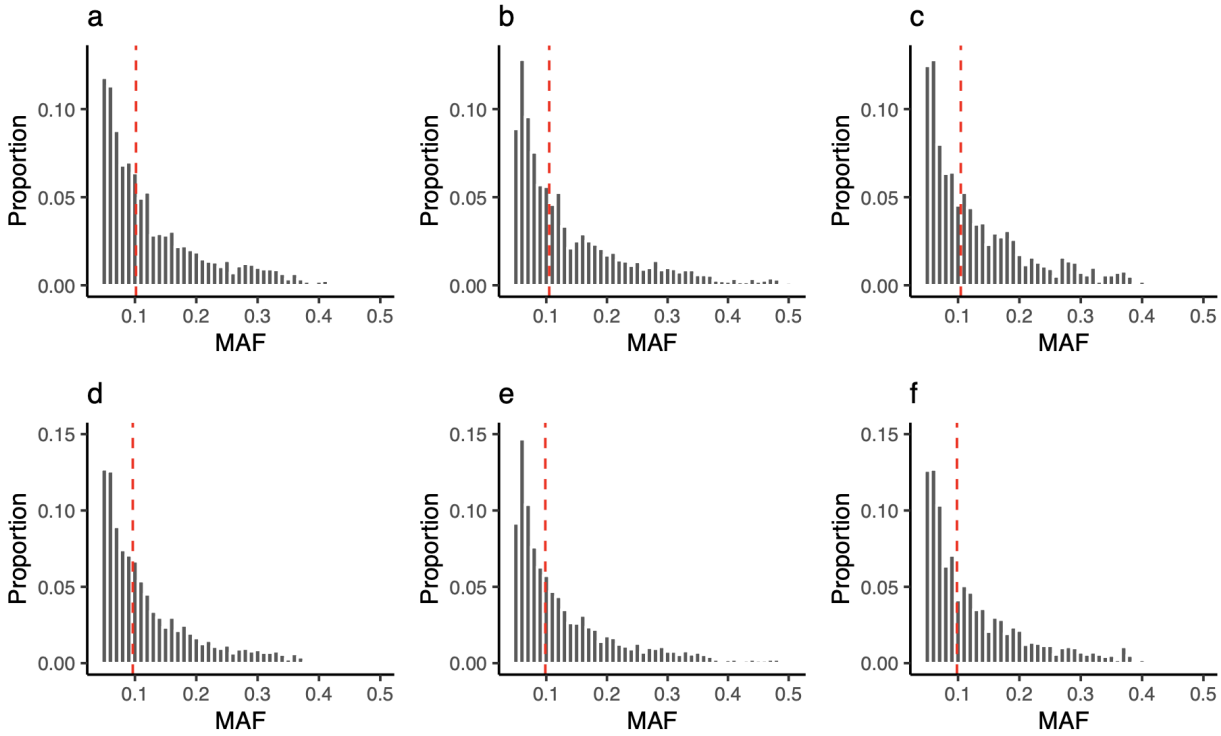

323

324 **Fig 4. Distribution of MAFs of eQTLs in male leaf (a, d), female leaf (b, e), pollen (c, f) in**
325 ***Rumex hastatulus*.** a-c: top eQTL per eGene, d-e: a randomly selected eQTL per eGene.
326 Binwidth = 0.01. Median MAF in each plot: 0.1017 (a), 0.1048 (b), 0.1045 (c), 0.0965 (d),
327 0.0984 (e), 0.0982 (f).

328

329 To investigate whether the patterns of excessive rare alleles in eQTLs suggested a signature of
330 genome-wide purifying selection, we compared the MAFs of true positive eQTLs to a null
331 distribution in each tissue (**Fig 5a-c**). We generated the null distributions of MAFs using 'false-
332 positive' eQTLs from permuted data by breaking the true assignment of individuals and re-

333 assigning their expression phenotypes. We then used the same procedure to identify false-
334 positive eQTLs from permuted data and true positive eQTLs from observed data (see Methods).
335 In all tissues we found an excess of rare alleles (MAF between 0.05 and 0.1) in the permuted
336 data compared to our observed data, with a small overlap in the proportions of rare alleles in
337 pollen (**Fig 5a-c**), suggesting that eQTLs do not show a genome-wide signature of purifying
338 selection.

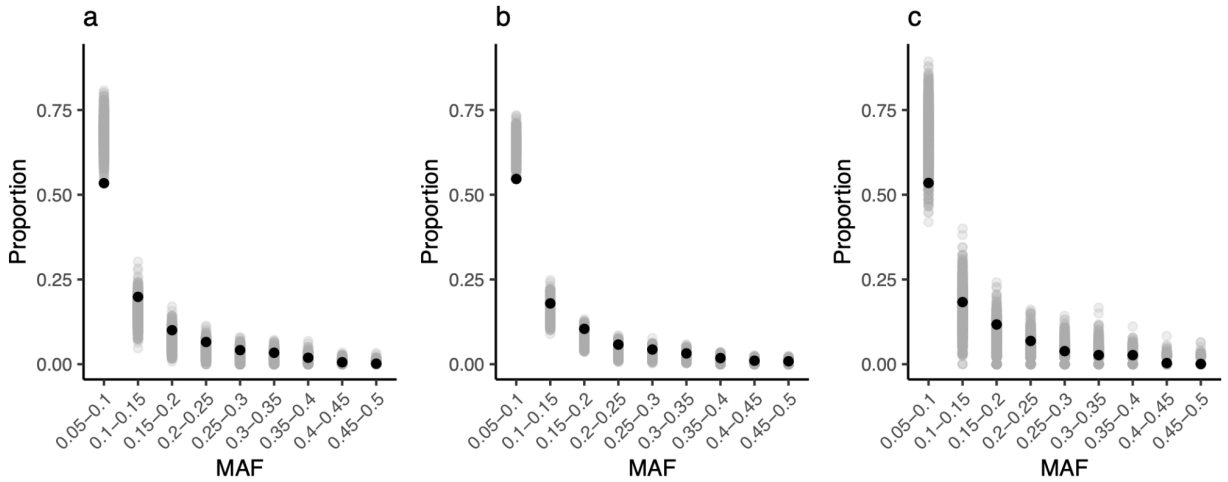

339

340 **Fig 5. Distribution of MAFs of eQTLs compared to a null distribution in male leaf (a),**
341 **female leaf (b) and pollen in *Rumex hastatulus.*** (c). Black dots: true positive eQTLs (observed
342 data), grey dots: false positive eQTLs (permuted data).

343

344 We identified 111 eGenes with 714 eQTLs in the PAR, and 1,294 eGenes with 16,112 eQTLs in
345 the X-specific regions in female leaf and compared their selective pressure using MAFs. The
346 MAFs of eQTLs in PAR and the X-specific regions showed an excess of rare alleles similar to
347 the autosomes (S8 Fig). We found eQTLs in the X-specific regions had significantly lower
348 MAFs than in autosomes using both methods of eQTL selection (Mann-Whitney *U*-test, $p <$
349 0.004), and eQTLs on PAR had significantly higher MAFs than the X-specific regions only in
350 top eQTLs (Mann-Whitney *U*-test, $p = 0.019$). However, the null distribution of MAFs of eQTLs
351 for X and autosomes did not differ significantly (S9 Fig); there were not enough false-positive
352 eQTLs in the PAR for comparison.

353

354 We compared MAFs of eQTLs shared between life stages and those that were life-stage specific.
355 We found shared eQTLs had significantly higher MAFs than specific eQTLs (Mann-Whitney *U*-

356 test, $p < 10^{-7}$), with a median MAFs of 0.143 and 0.093, respectively. Due to a lack of shared
357 false positive eQTLs between life stages, this result was not confirmed by a comparison to a null
358 distribution. We also tested signatures of selection on eGenes that were shared between sexes or
359 life stages using neutral diversity statistics. We predicted that shared eGenes would have higher
360 π and Tajima's D than specific eGenes, due to the greater potential for conflict in shared eGenes.
361 We found that shared eGenes between sexes had significantly higher Tajima's D (Kruskal-Wallis
362 test, $p < 10^{-5}$) but not significantly higher π (Kruskal-Wallis test, $p = 0.5383$) than male- or
363 female-specific eGenes. There were no significant differences in π or Tajima's D among shared
364 and specific eGenes in either life stage (ANOVA test, $p = 0.611$, 0.157, respectively).
365 Additionally, we tested the signature of selection on eGenes whose expression differences
366 between life stages were affected by eQTLs and found these eGenes had significantly higher π
367 and Tajima's D than eGenes not significant for expression differences (t-test, $p = 0.00013$,
368 0.00058, respectively).
369
370 **Discussion**
371 In this study we mapped *cis*-eQTLs in leaf and pollen tissues in the dioecious plant *R. hastatulus*
372 to test the scope for conflict between sexes and life stages, based on shared genetic architecture.
373 We investigated the overlap of eQTLs between sexes and life stages and examined their effect
374 sizes and allele frequencies. We discovered a much larger overlap in eGenes and eQTLs between
375 sexes than between life stages. For SNPs tested in both sexes or life stages, there was a stronger
376 correlation of effect sizes between sexes, which further suggests a more shared genetic
377 architecture between sexes than life stages. There were more minor alleles of eQTLs driving than
378 constraining divergent expression between life stages. Among the eQTLs shared between life
379 stages and affecting their expression differences, most minor alleles changed expression in the
380 same direction with different magnitudes, increasing the degree of divergent expression. MAFs
381 of eQTLs in all tissues exhibited similar distributions with an excess of rare alleles, but this
382 pattern did not reflect an excess of rare variants when compared to a null distribution. Below we
383 discuss the implications of our results on the extent of a shared genetic basis between sex and life
384 stages and also the use of eQTL mapping in testing evolutionary forces shaping *cis*-regulatory
385 variation.
386

387 *Potential for conflict between sexes and life stages*
388 With the potential for both sexual and life-stage conflict based on theory [6,7,41], key open
389 questions remain on whether there are more opportunities for conflict between sexes or life
390 stages, and whether sexual and life-stage conflict is still an ongoing process or has already
391 become resolved. We investigated this question using *cis*-regulatory variation which has a strong
392 effect on gene expression. Our results consistently suggested significantly more shared genetic
393 architecture between sexes than life stages, thus more potential for ongoing sexual conflict. In
394 contrast, our results indicate that life-stage conflict is more resolved compared to sexual conflict.
395 This finding is consistent with previous work suggesting considerable scope for ongoing sexual
396 conflict based on intersexual genetic covariances in expression [20–22]. The alternating life
397 cycle of diploid and haploid life stages is shared among all land plants, allowing them to adapt to
398 varying environments during their lives. This fundamental feature of alternation of generations
399 predates the evolution of dioecy in flowering plants, which has more recently emerged from
400 hermaphroditic ancestors in most lineages [42]. In dioecious plants such as *R. hastatulus*, it is
401 likely that there has been much more time to resolve conflict between life stages than sexes,
402 while in contrast, sexual conflict may still be ongoing. It is also worth mentioning that standing
403 variation in gene regulation might have more sex-differential effects in reproductive tissues such
404 as flowers compared to leaves. Future studies should benefit from a more diverse sampling of
405 both vegetative and reproductive tissues than we used in this study [31].
406
407 With a weak positive correlation of eQTL effect sizes between life stages, there is still potential,
408 albeit weaker, for ongoing life-stage conflict. Our previous study tested the genomic signature of
409 intra-locus conflict between life stages in *R. hastatulus* but did not find support for a genome-
410 wide signal [43]. Future studies with more functional understanding, e.g., on alleles beneficial
411 for pollen competition, combined with previously identified candidate genes under balancing
412 selection [43] should help to uncover the genetic basis of life-stage conflict in *R. hastatulus*.
413 Plants are useful systems for comparing opportunities for sexual and life-stage conflict compared
414 to animals; yet studies on selection and potential conflict between sexes or life stages in plants
415 are still very limited [5,12,13]. Whether there are differences in the possibilities for sexual and
416 life-stage conflict in plants with different sexual systems (hermaphroditic vs. dioecious) or
417 different types of life cycles (predominantly diploid vs. haploid) would certainly be worth further
418 investigation.

419

420 *Selective pressure on cis-regulatory variation*

421 Estimating selective pressures in regulatory variation using allele frequencies has resulted in
422 mixed results supporting contrasting hypotheses about the type of selection on *cis*-eQTLs
423 [25,29]. Our results indicated more rare than common alleles among cis-eQTLs in all tissues.
424 However, in contrast to our prediction and previous findings in *Capsella grandiflora* [25], there
425 was a marginally higher proportion of rare alleles in the null distribution than our observed data,
426 suggesting a genome-wide signature of purifying selection was unlikely. With the *cis*-eQTLs in
427 *Mimulus* floral tissues showing an excess of common alleles [29], it is unclear whether *cis*-
428 regulatory variation is generally subject to purifying selection based on their allele frequencies.
429 Conserved non-coding regions are often constrained due to their putative regulatory functions
430 [44,45]; excessive rare alleles in cis-eQTLs were found in the promoter regions of yeast [46].
431 Notably, selection on noncoding sequences in plants is rarer than in animals [47], due to low
432 complexity of regulatory regions on a per gene basis [48]. Investigation of the burden of rare
433 alleles on genotypes with more extreme gene expression [49] could be a promising next step that
434 might be more powerful than comparing genome-wide allele frequency spectra to a null
435 distribution. Future studies should also benefit from examining the correlation between effect
436 sizes and MAFs while controlling for confirmation bias using allele-specific eQTLs [25] and
437 also examining trans-eQTLs as they are subject to stronger constraint than *cis*-acting variation
438 [28].

439

440 In addition to testing selective pressures on eQTLs based on allele frequencies, we examined
441 signatures of selection on eGenes using diversity statistics. We expected eQTLs with concordant
442 effects between sexes or life stages to experience stronger conflict than eQTLs with discordant
443 effects (assuming fitness effects of expression are concordant between sexes or life stages) or
444 eQTLs exclusive to one sex or life stage. We only found that shared eGenes had higher Tajima's
445 *D* than sex-specific eGenes. In contrast to our prediction, eGenes with eQTLs affecting their
446 expression differences between life stages had significantly higher π and Tajima's *D* than eGenes
447 not significant for expression differences; however, this finding might result from an
448 ascertainment bias, as it is more likely to have higher power to detect interactions when diversity
449 is higher. Overall, we did not find a compelling signal of past conflict between sexes or life
450 stages in eQTLs. Detecting balancing selection due to conflict using genomic data remains a

451 challenging problem [50,51]. Additionally, previous work has shown that sexually concordant
452 selection also plays an equally important role in shaping sexual dimorphism in expression [22].
453 Combined with our previous results on the widespread synergistic pleiotropy between life stages
454 from population genomic data [43], out findings in this study suggest that concordant selection is
455 likely more prevalent and/or detectable than antagonistic selection in genome-wide studies.
456

457 **Methods**

458 *Plant materials*

459 We described the details of plant materials and sequencing in [43]; here we provide a brief
460 summary and additional relevant information. After generating seedlings using open-pollinated
461 seeds collected from a population in Rosebud, Texas, US [34], we paired one female and male
462 individual randomly at the time of flowering for crossing and collected seeds to generate F_1
463 plants. We planted and retained multiple individuals per family for 78 F_1 families to ensure we
464 had one male-female full sibling pair per family for tissue collection. We collected leaf tissue
465 from each male-female full-sibling pair for both RNA and DNA sequencing and collected
466 mature pollen grains from males for RNA sequencing. We described the DNA and RNA
467 isolation protocols in [43]. The DNA samples were sequenced at a depth of 10-15X. Raw
468 sequences of male leaf RNA and pollen RNA were described in [43], Initial sample sizes for
469 DNA samples and female leaf RNA samples are presented in Table S1.
470

471 *DNA Seq data and variant calling*

472 We used a phased PacBio genome assembly consisting of four autosomes, X-specific, Y-specific
473 and pseudoautosomal regions for our analyses [38]. We mapped the DNA reads to the genome
474 assembly and added read groups using bwa-mem2 [52]. We sorted the BAM, marked PCR
475 duplicates and indexed the final BAM using SAMTools [53]. We called variants in parallel on 2
476 Mb non-overlapping contigs of each chromosome for all samples using BCFtools mpileup [53],
477 then concatenated the VCFs of contigs for each chromosome. We removed one male sample
478 (24fM) due to low genomic coverage and two samples due to incorrect sex labeling (35aM,
479 40aF), and only kept samples with both DNA and RNA sequences from the same individual. For
480 males, we only kept samples with both leaf and pollen RNA sequences from the same individual.
481 Our sample sizes for VCF filtering were 74 for female leaf, 73 for male leaf, making a total of
482 147 leaf tissue samples. We performed SNP filtering as follows for female leaf, male leaf and all

483 leaf samples combined separately using VCFtools [54]. We kept SNPs with QUAL > 30, a mean
484 depth between 5 and 20, a genotype quality per sample > 30 otherwise marked as missing, and
485 finally a missingness < 20%. For female samples, we used the same filtering criteria for
486 autosomes, PAR and X-specific regions. The numbers of autosomal SNPs were 64,988,762 in
487 male leaf, 66,828,708 in female leaf, and 66,341,762 in all leaf samples combined. The numbers
488 of SNPs on X-specific regions and PAR in females were 7,745,941 and 2,164,214, respectively.
489 Additionally, we filtered for invariant sites on autosomes with a mean depth between 5 and 20
490 and a missingness < 20% for all leaf samples combined.
491
492 We removed SNPs with a minor allele frequency lower than 5% or with strong Hardy–Weinberg
493 deviations ($p < 10^{-6}$) on autosomes using Plink [55] to test for population structure and for the
494 subsequent eQTL mapping. We removed four male samples (7bM, 27eM, 53bM, 5aM) from
495 subsequent analyses for being outliers in principal component analyses in Plink [55]. Our final
496 sample sizes were 74 for female leaf, 69 for male leaf, making a total of 143 leaf samples. After
497 the filtering using Plink, the numbers of SNPs on autosomes were 3,288,995 in male leaf,
498 4,509,904 in female leaf, and 3,684,937 in all leaf samples combined; the numbers of SNPs on
499 X-specific regions and PAR in females were 769,059 and 96,911, respectively.
500
501 *RNA Seq data and expression analyses*
502 We mapped the RNA reads to our genome assembly in a two pass mode, sorted the BAM files
503 by coordinates, added read groups using STAR [56], and indexed the output BAM files using
504 SAMTools [53]. We generated read counts for each gene using featureCount [57]. We only kept
505 genes with evidence of expression for our subsequent analyses, i.e., genes with a mean raw read
506 count ≥ 5 in a specific tissue, or in at least one tissue for analyses involving both sexes or life
507 stages. We identified sex-biased genes in leaf tissues and life-stage-biased genes by comparing
508 pollen and male leaf tissues using DESeq2 [58]. The cutoffs for significant differentially
509 expressed (DE) genes were Benjamini-Hochberg adjusted $p < 0.05$ and fold change > 2 unless
510 stated otherwise.
511
512 We prepared the expression phenotype data for each tissue separately and for all leaf samples
513 combined for eQTL mapping. We normalized raw read counts by sequencing depth using

514 DESeq2 [58] and performed quantile normalization in R [59]. Additionally, we calculated the
515 difference of normalized read counts in pollen and male leaf (male leaf minus pollen) for each
516 gene and performed quantile normalization of its absolute value in R [59].
517
518 *Correlation in gene expression*
519 To characterize the correlation in expression across life stages or sexes, we used Pearson
520 correlations and the final normalized read counts as expression level as described above. For
521 male leaves and pollen, we calculated the correlation of a given gene's expression level in each
522 tissue using 69 male individuals and repeated for 16,411 autosomal genes that had evidence of
523 expression (as described above) to generate a distribution of correlations. These correlations are
524 the same as any phenotypic correlation in behavioral or morphological traits, but for gene
525 expression [60]. To estimate the across-sex correlation in expression, we took advantage of the
526 sib-structure of our design and the fact that we had male and female sibling pairs. We used the
527 expression level of a gene in a male sample and its female sibling as a pair of observations,
528 repeated for 64 sibling pairs in our design, to estimate the correlation in expression across
529 siblings for a given gene. We then repeated this for 14,992 genes with evidence of expression in
530 the samples to generate a distribution of across-sex correlation in expression. Note that because
531 we only had a single male and female sample per family, rather than replicates, this is a
532 phenotypic approximation of the across-sex genetic correlation (r_{mf}), rather than a genetic
533 correlation. We repeated the analyses for genes regulated by eQTLs (eGenes, see below) in at
534 least one life stage or sex following the same steps.
535
536 *eQTL mapping*
537 We performed *cis*-eQTL mapping on autosomes separately for male leaf, female leaf, and pollen
538 tissue. For female leaf, we repeated eQTL mapping on X and PAR using the same approach as
539 the autosomes. For male samples, we performed eQTL mapping using the difference in leaf and
540 pollen expression levels as phenotypes in the same way as in leaf or pollen separately. To
541 control for genetic relatedness, we performed LD pruning in Plink [55] and identified genetic
542 principal components (PC) using EIGENSOFT smartpca [61,62]. The significance of each PC
543 was determined by the Tracy-Widom test [61,63]. We included the significant PCs ($p < 0.05$) as
544 covariates in eQTL mapping.
545

546 We mapped *cis*-eQTL using tensorQTL [64] following its guidelines, and tested pre linkage-
547 pruning SNPs within a 20 kb window to the transcription start site for each gene. We performed
548 adaptive permutations to calculate empirical and beta-approximated empirical *p*-values for each
549 gene [65], and generated nominal *p*-values for all SNP-gene pairs. We calculated the Storey *q*-
550 value and the nominal *p*-value threshold for significant associations based on the beta-
551 approximated empirical *p*-value for each gene using a false discovery rate (FDR) of 0.1 [66,67].
552 We filtered for genes that had *q*-value < 0.1 and at least one eQTL as our eGenes. We filtered for
553 SNPs with a nominal *p*-value smaller than the nominal *p*-value threshold of its eGene as our
554 eQTLs. The minimum *p*-value threshold is 0.0318 for male leaf, 0.0503 for female leaf, and
555 0.0166 for pollen. We identified conditionally independent eQTLs for eGenes using a forward-
556 backward stepwise regression model in tensorQTL [68]. We defined primary eQTLs as the top
557 ranked eQTL for each eGene, and any additionally ranked eQTLs as secondary or conditionally
558 independent eQTLs. The effect size of an eQTL was defined as the slope in the linear regression
559 model from tensorQTL.
560
561 We kept one eQTL for every eGene, either the most significant (top) eQTL or a randomly
562 selected eQTL when comparing minor allele frequencies (MAF) and when testing the
563 relationship between effect size and the distance to transcription start site of eQTLs. We
564 removed eQTLs and eGenes when an eQTL affected multiple eGenes when comparing MAFs.
565 We performed gene ontology enrichment of eGenes using topGO [69], significant GO terms
566 were selected using a *p*-value cutoff of 0.05 based on Fisher's exact tests. To test for the
567 enrichment of expression bias categories among genes whose expression differences between life
568 stages were affected by eQTLs, we grouped DE gene into four bins based on the absolute value
569 of $\log_2$FoldChange (≤ 1, >1 and ≤2, >2 and ≤3, >3) and performed Chi-squared test, where
570 positive Pearson residuals indicate enrichment and negative residuals indicate
571 underrepresentation.
572
573 We ran tensorQTL on all 143 leaf samples to test the linear model: Expression ~ Genotype + Sex
574 + Genotype × Sex. We kept the top association for each gene based on the interaction term (-best
575 only), and calculated multiple-testing corrected [39] and Benjamini-Hochberg adjusted *p*-values
576 (pval_adj_bh) following the recommendations from tensorQTL. The cutoff for eQTLs showing
577 significant Genotype × Sex is pval_adj_bh < 0.1.

578

579 *Null distributions of eQTL MAFs*

580 To generate a null distribution for MAFs of eQTLs in each tissue, we performed permutations by
581 randomly re-assigning sample ID's in the expression phenotype file. We performed 1000
582 permutations in both females and males. For female leaves, we performed the same permutations
583 on X and PAR as the autosomes. For male samples, we performed permutations the same way in
584 male leaf and pollen phenotypes and identified the shared and specific eQTLs between male leaf
585 and pollen in each permutation. We identified false-positive eQTLs using the same *p*-value
586 thresholds from the previous analyses on our observed data. We removed eGenes with more than
587 10 eQTLs, randomly selected an eQTL from each eGene, and removed eQTLs affecting multiple
588 eGenes. We repeated the same procedure of calculating MAF using true positive eQTLs. The
589 proportions of false positive eGenes compared to true positive eGenes were 0.059 in male leaf,
590 0.105 in female leaf, and 0.0318 in pollen, based on the median number of false positive eGenes
591 in 1000 permutations.

592

593 *Diversity statistics*

594 We used the script codingSiteTypes.py
595 (https://github.com/simonhmartin/genomics_general/blob/master/codingSiteTypes.py, accessed
596 in 2020) to extract 4-fold degenerate site for calculating neutral diversity statistics. We generated
597 4-fold VCFs including both variant and invariant sites using all leaf samples combined. We used
598 pixy [70,71] to calculate nucleotide diversity (π) and Tajima's *D* for all autosomal genes. We
599 only kept genes with at least 50 sites in the subsequent analyses of π and Tajima's *D*. We
600 removed genes if they were associated with an eQTL that affected multiple eGenes.

601

602 **Data availability**

603 Raw sequencing reads are available through the NCBI SRA database under BioProject
604 PRJNA744278 to be released on August 1, 2025. Scripts and data used to generate the figures
605 are available at https://github.com/SIWLab/Rumex_eQTL.

606

Acknowledgement

We thank Yunchen Gong for technical assistance with the computing servers and Bill Cole and Thomas Gludovacz for help with plant maintenance. This study was supported by NSERC Discovery Grants awarded to SCHB, JRS and SIW.

References

1. Ewing EP. Selection at the haploid and diploid phases: cyclical variation. Genetics. 1977;87: 195–207.

2. Arnqvist G, Rowe L. Sexual conflict. Princeton University Press; 2005.

3. Haig D, Wilczek A. Sexual conflict and the alternation of haploid and diploid generations. Philos Trans R Soc B Biol Sci. 2006;361: 335–343.

4. Schärer L, Janicke T, Ramm SA. Sexual conflict in hermaphrodites. Cold Spring Harb Perspect Biol. 2015;7: a017673.

5. Beaudry FEG, Rifkin JL, Barrett SCH, Wright SI. Evolutionary genomics of plant gametophytic selection. Plant Commun. 2020;1: 100115.

6. Kidwell JF, Clegg MT, Stewart FM. Regions of stable equilibria for models of differential selection in the two sexes under random mating. Genetics. 1976;85: 171–183.

7. Immler S, Arnqvist G, Otto SP. Ploidally antagonistic selection maintains stable genetic polymorphism: ploidally antagonistic selection. Evolution. 2012;66: 55–65.

8. Travers SE, Mazer SJ. Trade-offs between male and female reproduction associated with allozyme variation in phosphoglucoisomerase in an annual plant (*Clarkia unguiculata*: Onagraceae). Evolution. 2001;55: 2421–2428.

9. Lankinen A, Kiboi S. Pollen donor identity affects timing of stigma receptivity in *Collinsia heterophylla* (Plantaginaceae): a sexual conflict during pollen competition? Am Nat. 2007;170: 854–863.

10. Madjidian JA, Lankinen Å. Sexual conflict and sexually antagonistic coevolution in an annual plant. PLOS ONE. 2009;4: e5477.

11. Lankinen Å, Hydbom S, Strandh M. Sexually antagonistic evolution caused by male–male competition in the pistil. Evolution. 2017;71: 2359–2369.

12. Prasad NG, Bedhomme S. Sexual conflict in plants. J Genet. 2006;85: 161–164.

13. Moore JC, Pannell JR. Sexual selection in plants. Curr Biol CB. 2011;21: R176-182.

14. Duffy KJ, Mdlalose ZM, Johnson SD. Sexual conflict in hermaphroditic flowers of an African aloe. Int J Plant Sci. 2021;182: 238–243.

640 15. Delph LF, Arntz AM, Scotti Saintagne C, Scotti I. The genomic architecture of sexual
641 dimorphism in the dioecious plant *Silene latifolia*. Evolution. 2010;64: 2873–2886.

642 16. Lande R. Sexual dimorphism, sexual selection, and adaptation in polygenic characters.
643 Evolution. 1980;34: 292.

644 17. Poissant J, Wilson AJ, Coltman DW. Sex-specific genetic variance and the evolution of
645 sexual dimorphism: a systematic review of cross-sex genetic correlations. Evolution.
646 2010;64: 97–107.

647 18. Wyman MJ, Stinchcombe JR, Rowe L. A multivariate view of the evolution of sexual
648 dimorphism. J Evol Biol. 2013;26: 2070–2080.

649 19. Mank JE. The transcriptional architecture of phenotypic dimorphism. Nat Ecol Evol.
650 2017;1: 0006.

651 20. Innocenti P, Morrow EH. The sexually antagonistic genes of *Drosophila melanogaster*.
652 Hurst LD, editor. PLoS Biol. 2010;8: e1000335.

653 21. Griffin RM, Dean R, Grace JL, Rydén P, Friberg U. The shared genome is a pervasive
654 constraint on the evolution of sex-biased gene expression. Mol Biol Evol. 2013;30: 2168–
655 2176.

656 22. Houle D, Cheng C. Predicting the evolution of sexual dimorphism in gene expression. Mol
657 Biol Evol. 2021;38: 1847–1859.

658 23. Kudaravalli S, Veyrieras J-B, Stranger BE, Dermitzakis ET, Pritchard JK. Gene expression
659 levels are a target of recent natural selection in the human genome. Mol Biol Evol. 2009;26:
660 649–658.

661 24. Lee YW, Gould BA, Stinchcombe JR. Identifying the genes underlying quantitative traits: a
662 rationale for the QTN programme. AoB PLANTS. 2014;6.

663 25. Josephs EB, Lee YW, Stinchcombe JR, Wright SI. Association mapping reveals the role of
664 purifying selection in the maintenance of genomic variation in gene expression. Proc Natl
665 Acad Sci. 2015;112: 15390–15395.

666 26. Josephs EB, Stinchcombe JR, Wright SI. What can genome-wide association studies tell us
667 about the evolutionary forces maintaining genetic variation for quantitative traits? New
668 Phytol. 2017;214: 21–33.

669 27. Signor AS, Nuzhdin SV. The evolution of gene expression in *cis* and *trans*. Trends in
670 Genetics. 2018;34(7):532-44.

671 28. Josephs EB, Lee YW, Wood CW, Schoen DJ, Wright SI, Stinchcombe JR. The
672 evolutionary forces shaping *cis*- and *trans*-regulation of gene expression within a
673 population of outcrossing plants. Mol Biol Evol. 2020;37: 2386–2393.

674 29. Brown KE, Kelly JK. Genome-wide association mapping of transcriptome variation in

675 *Mimulus guttatus* indicates differing patterns of selection on *cis*- versus *trans*-acting
676 mutations. Genetics. 2021;220: iyab189.

677 30. Oliva M, Muñoz-Aguirre M, Kim-Hellmuth S, Wucher V, Gewirtz ADH, Cotter DJ, et al.
678 The impact of sex on gene expression across human tissues. Science. 2020;369.

679 31. Puixeu G, Macon A, Vicoso B. Sex-specific estimation of *cis* and *trans* regulation of gene
680 expression in heads and gonads of *Drosophila melanogaster*. G3 GenesGenomesGenetics.
681 2023;13: jkad121.

682 32. Mishra P, Barrera TS, Grieshop K, Agrawal AF. *Cis*-regulatory variation in relation to sex
683 and sexual dimorphism in *Drosophila melanogaster*. Genome Biol Evol. 2024;16: evae234.

684 33. Field DL, Pickup M, Barrett SCH. Ecological context and metapopulation dynamics affect
685 sex-ratio variation among dioecious plant populations. Ann Bot. 2013;111: 917–923.

686 34. Pickup M, Barrett SCH. The influence of demography and local mating environment on sex
687 ratios in a wind-pollinated dioecious plant. Ecol Evol. 2013;3: 629–639.

688 35. Hough J, Hollister JD, Wang W, Barrett SCH, Wright SI. Genetic degeneration of old and
689 young Y chromosomes in the flowering plant *Rumex hastatulus*. Proc Natl Acad Sci.
690 2014;111: 7713–7718.

691 36. Crowson D, Barrett SCH, Wright SI. Purifying and positive selection influence patterns of
692 gene loss and gene expression in the evolution of a plant sex chromosome system. Mol Biol
693 Evol. 2017;34: 1140–1154.

694 37. Sandler G, Beaudry FEG, Barrett SCH, Wright SI. The effects of haploid selection on Y
695 chromosome evolution in two closely related dioecious plants. Evol Lett. 2018;2: 368–377.

696 38. Sacchi BM, Yuan M, Pyne C, Choudhury BI, Gong Y, Barrett SCH, et al. Early regulatory
697 evolution contributes to Y chromosome degeneration in *Rumex hastatulus* [unpublished
698 manuscript]. 2025

699 39. Davis JR, Fresard L, Knowles DA, Pala M, Bustamante CD, Battle A, et al. An efficient
700 multiple-testing adjustment for eQTL studies that accounts for linkage disequilibrium
701 between variants. Am J Hum Genet. 2016;98: 216–224.

702 40. Tajima F. Statistical method for testing the neutral mutation hypothesis by DNA
703 polymorphism. Genetics. 1989;123: 585.

704 41. Peters MAE, Weis AE. Isolation by phenology synergizes isolation by distance across a
705 continuous landscape. New Phytol. 2019;224: 1215–1228.

706 42. Bawa KS. Evolution of dioecy in flowering plants. Annu Rev Ecol Syst. 1980;11: 15–39.

707 43. Yuan M, Kollar LM, Sacchi BM, Carey SB, Choudhury BI, Jones T, et al. Testing for the
708 genomic footprint of conflict between life stages in an angiosperm and a moss species.
709 bioRxiv [Preprint]. 2025. Available from:

710 https://www.biorxiv.org/content/10.1101/2024.10.04.613734v2

711 44. Casillas S, Barbadilla A, Bergman CM. Purifying selection maintains highly conserved
712 noncoding sequences in *Drosophila*. Mol Biol Evol. 2007;24: 2222–2234.

713 45. Haudry A, Platts AE, Vello E, Hoen DR, Leclercq M, Williamson RJ, et al. An atlas of over
714 90,000 conserved noncoding sequences provides insight into crucifer regulatory regions.
715 Nat Genet. 2013;45: 891–898.

716 46. Ronald J, Akey JM. The evolution of gene expression QTL in *Saccharomyces cerevisiae*.
717 PLOS ONE. 2007;2: e678.

718 47. Williamson RJ, Josephs EB, Platts AE, Hazzouri KM, Haudry A, Blanchette M, et al.
719 Evidence for widespread positive and negative selection in coding and conserved
720 noncoding regions of *Capsella grandiflora*. PLoS Genet. 2014;10: e1004622.

721 48. Lockton S, Gaut BS. Plant conserved non-coding sequences and paralogue evolution.
722 Trends Genet. 2005;21: 60–65.

723 49. Uzunović J, Josephs EB, Stinchcombe JR, Wright SI. Transposable elements are important
724 contributors to standing variation in gene expression in *Capsella grandiflora*. Mol Biol
725 Evol. 2019;36: 1734–1745.

726 50. Flintham E, Savolainen V, Otto SP, Reuter M, Mullon C. The maintenance of genetic
727 polymorphism underlying sexually antagonistic traits. Evol Lett. 2025;9: 259–272.

728 51. Ruzicka F, Zwoinska MK, Goedert D, Kokko H, Richter X-YL, Moodie IR, et al. A century
729 of theories of balancing selection. bioRxiv [Preprint]. 2025. Available from:
730 https://www.biorxiv.org/content/10.1101/2025.02.12.637871v1

731 52. Vasimuddin M, Misra S, Li H, Aluru S. Efficient architecture-aware acceleration of BWA-
732 MEM for multicore systems. 2019 IEEE International Parallel and Distributed Processing
733 Symposium (IPDPS). 2019. pp. 314–324.

734 53. Danecek P, Bonfield JK, Liddle J, Marshall J, Ohan V, Pollard MO, et al. Twelve years of
735 SAMtools and BCFtools. GigaScience. 2021;10: giab008.

736 54. Danecek P, Auton A, Abecasis G, Albers CA, Banks E, DePristo MA, et al. The variant call
737 format and VCFtools. Bioinformatics. 2011;27: 2156–2158.

738 55. Chang CC, Chow CC, Tellier LC, Vattikuti S, Purcell SM, Lee JJ. Second-generation
739 PLINK: rising to the challenge of larger and richer datasets. GigaScience. 2015;4: s13742-
740 015-0047–8.

741 56. Dobin A, Davis CA, Schlesinger F, Drenkow J, Zaleski C, Jha S, et al. STAR: ultrafast
742 universal RNA-seq aligner. Bioinformatics. 2013;29: 15–21.

743 57. Liao Y, Smyth GK, Shi W. featureCounts: an efficient general purpose program for
744 assigning sequence reads to genomic features. Bioinforma Oxf Engl. 2014;30: 923–930.

745 58. Love MI, Huber W, Anders S. Moderated estimation of fold change and dispersion for
746 RNA-seq data with DESeq2. Genome Biol. 2014;15: 550.

747 59. R Core Team. R: a language and environment for statistical computing. 2022. Available
748 from: https://www.R-project.org/

749 60. Stinchcombe JR, Kelly JK. Measuring natural selection on the transcriptome. New Phytol.
750 In press.

751 61. Patterson N, Price AL, Reich D. Population structure and eigenanalysis. PLOS Genet.
752 2006;2: e190.

753 62. Price AL, Patterson NJ, Plenge RM, Weinblatt ME, Shadick NA, Reich D. Principal
754 components analysis corrects for stratification in genome-wide association studies. Nat
755 Genet. 2006;38: 904–909.

756 63. Sztepanacz JL, Blows MW. Accounting for sampling error in genetic eigenvalues using
757 random matrix theory. Genetics. 2017;206: 1271–1284.

758 64. Taylor-Weiner A, Aguet F, Haradhvala NJ, Gosai S, Anand S, Kim J, et al. Scaling
759 computational genomics to millions of individuals with GPUs. Genome Biol. 2019;20: 228.

760 65. Ongen H, Buil A, Brown AA, Dermitzakis ET, Delaneau O. Fast and efficient QTL mapper
761 for thousands of molecular phenotypes. Bioinformatics. 2016;32: 1479–1485.

762 66. Benjamini Y, Hochberg Y. Controlling the false discovery rate: a practical and powerful
763 approach to multiple testing. J R Stat Soc Ser B Methodol. 1995;57: 289–300.

764 67. Storey JD. A direct approach to false discovery rates. J R Stat Soc Ser B Stat Methodol.
765 2002;64: 479–498.

766 68. Aguet F, Brown AA, Castel SE, Davis JR, He Y, Jo B, et al. Genetic effects on gene
767 expression across human tissues. Nature. 2017;550: 204–213.

768 69. Alexa A, Rahnenfuhrer J. topGO: enrichment analysis for Gene Ontology. R package
769 version 2.50.0. Available from: https://bioconductor.org/packages/topGO

770 70. Korunes KL, Samuk K. pixy: Unbiased estimation of nucleotide diversity and divergence in
771 the presence of missing data. Mol Ecol Resour. 2021;21: 1359–1368.

772 71. Bailey N, Stevison L, Samuk K. Correcting for bias in estimates of θ_w and Tajima's *D* from
773 missing data in Next-Generation Sequencing. Mol Ecol Resour. 2025;e14104.

774 **Supplementary Tables**

775 S1 Table. DNA and RNA samples of *Rumex hastatulus* used in this study.

776 S2 Table. Number of DE genes in *Rumex hastatulus*.

777 S3 Table. GO enrichment of eGenes in male leaf, female leaf, and pollen of *Rumex hastatulus*.

778 S4 Table. GO enrichment of eGenes with discordant eQTLs between life-stages or sexes in

779 *Rumex hastatulus*.

780 S5 Table. GO enrichment of eGenes with discordant eQTLs for expression differences between

781 life-stages of *Rumex hastatulus*.

782

783 **Supplementary Figures**

784

785 S1 Fig. PCA of leaf and pollen RNA samples of *Rumex hastatulus*. a-b: male vs. female leaf. c-d:

786 pollen vs. male leaf. a,c: whole genome including X- and Y-specific regions, b,d: only

787 autosomes and PAR.

788

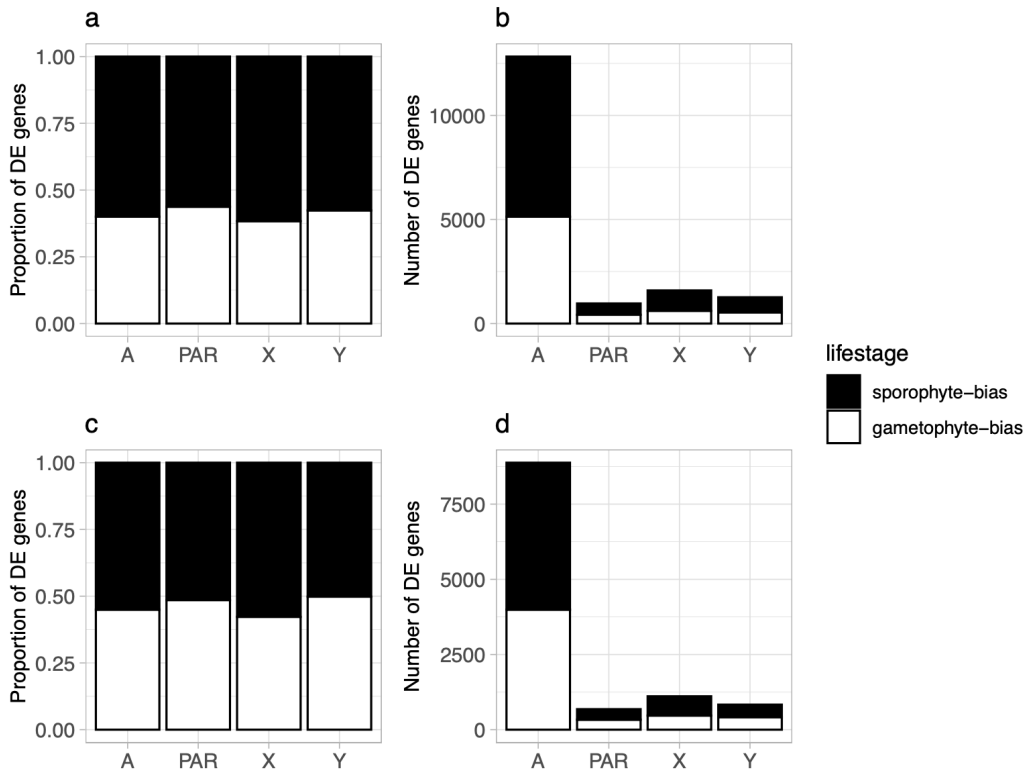

S2 Fig. Enrichment of gametophyte-biased genes on the sex chromosomes in *Rumex hastatulus.* Cutoff for DE genes: adjusted $p < 0.05$ and fold change > 2 (a, b), fold change > 4 (c, d).

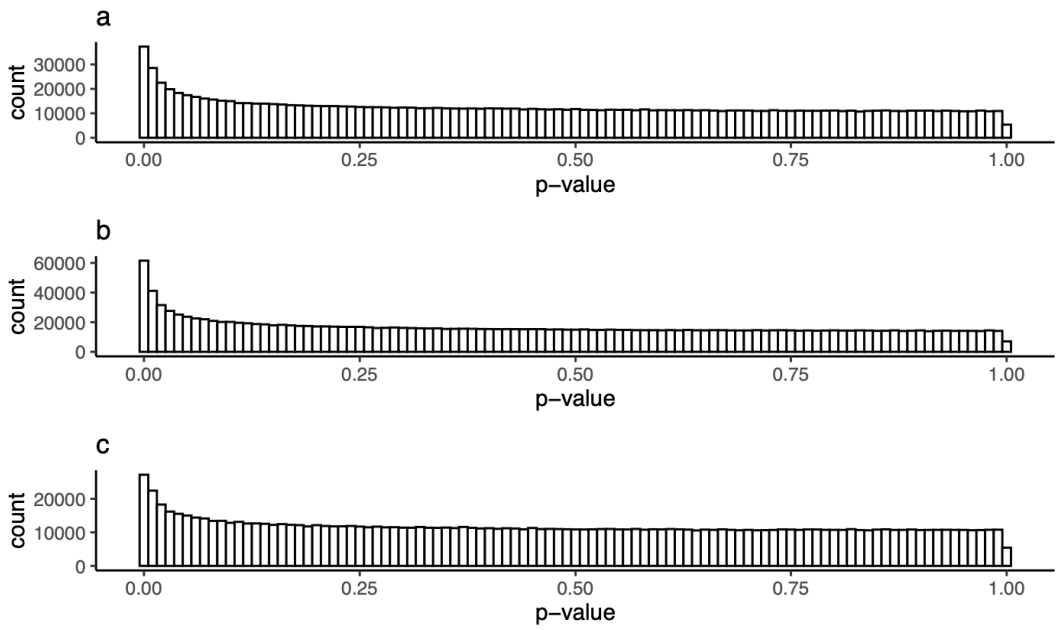

S3 Fig. Distribution of nominal *p*-values for all nearby SNPs tested in male leaf (a), female leaf (b), pollen (c) of *Rumex hastatulus*. Bin size = 0.01.

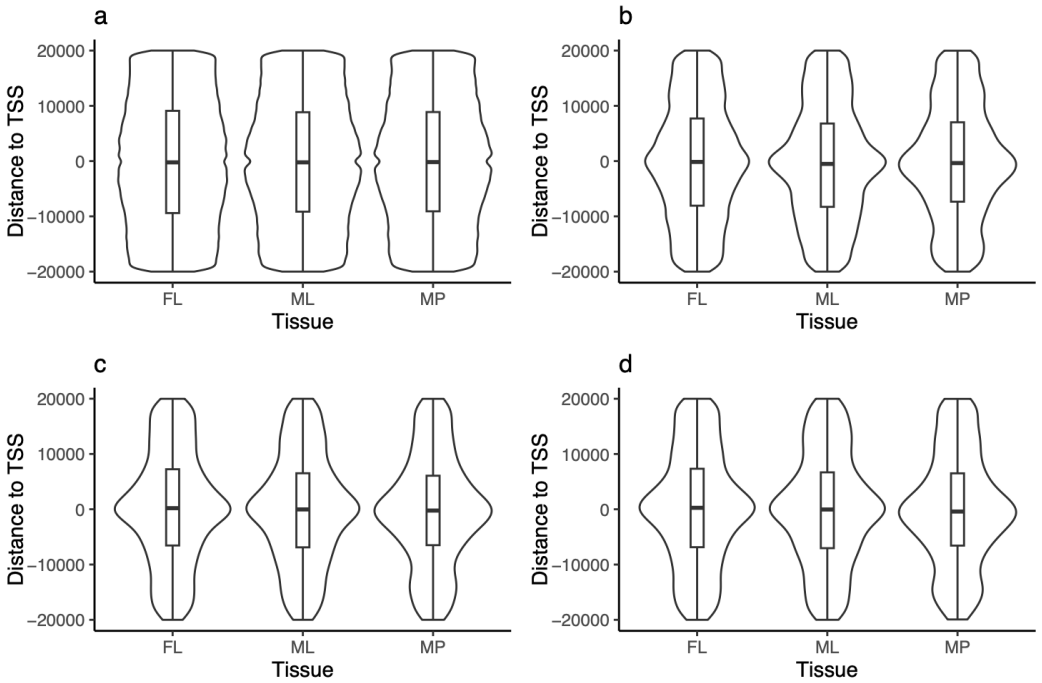

S4 Fig. Distance between eQTL and the transcription start site of eQTLs male leaf (ML), female leaf (FL), pollen (MP) of *Rumex hastatulus*. a. All nearby SNPs, b. all eQTLs, c. the most significant eQTL for each eGene, d. a randomly selected significant eQTL for each eGene.

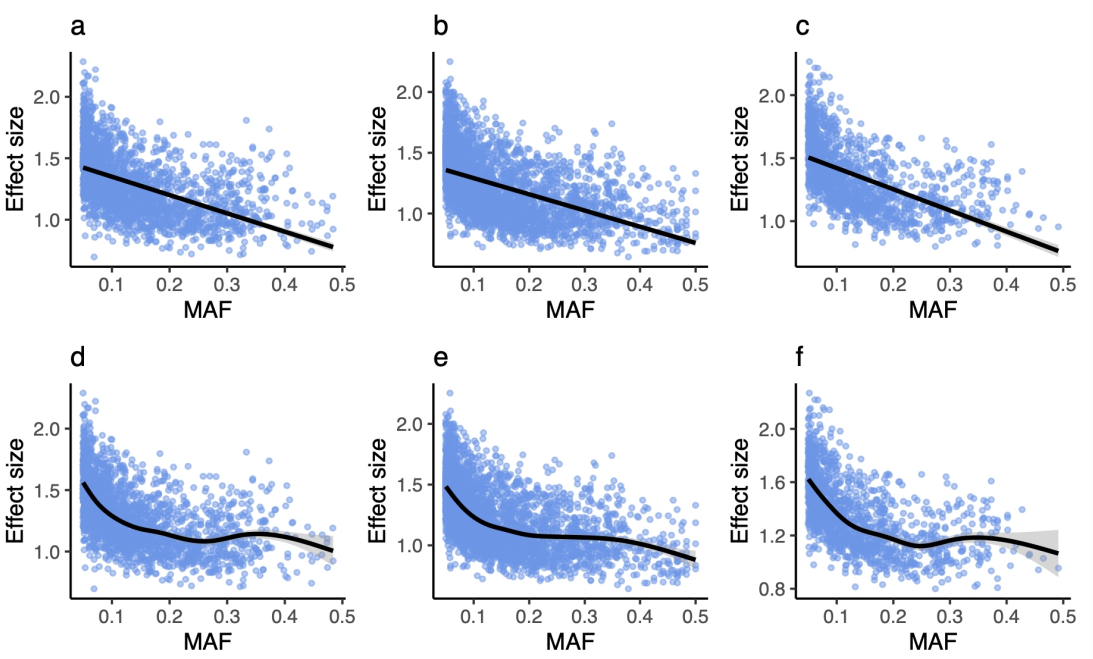

S5 Fig. Correlation between effect sizes and MAFs of eQTLs in male leaf (a, d), female leaf (b, e), and pollen (c, f) of *Rumex hastatulus*. Effect size is defined as the absolute value of the slope

804 in the linear models in eQTL mapping. a-c, linear regression, d-f: default smoothing function in
805 R.
806

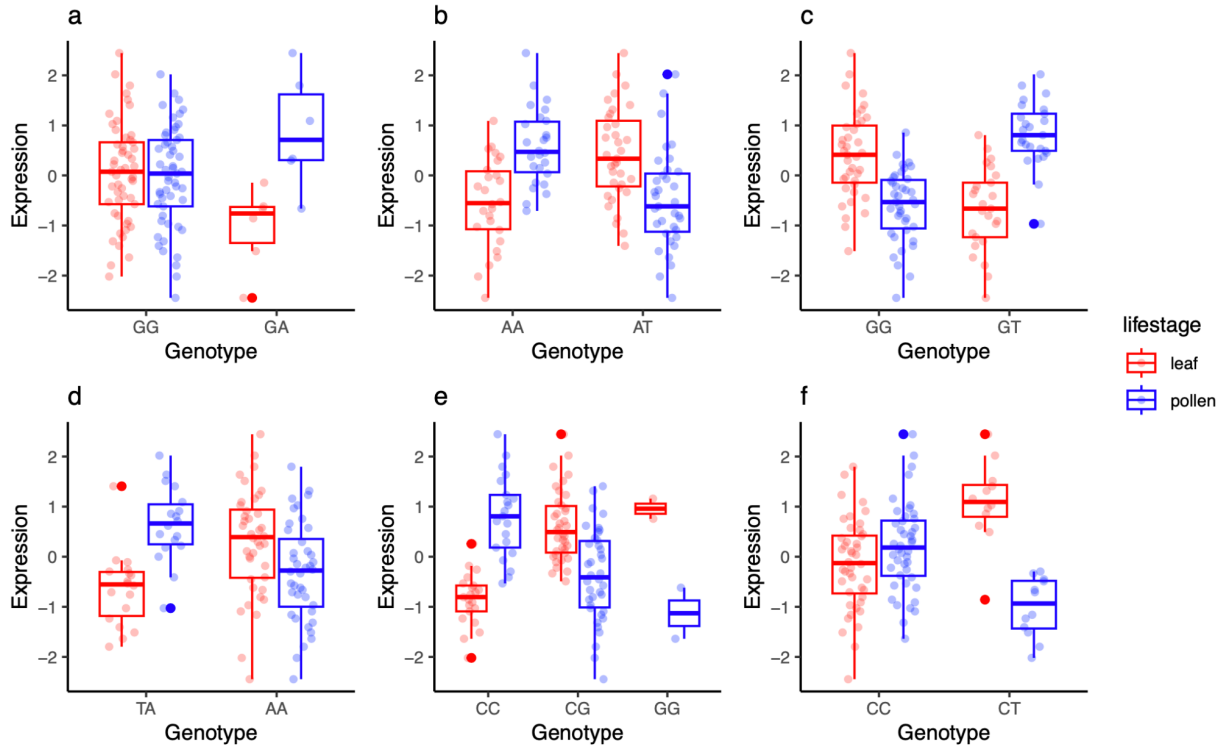

807
808 S6 Fig. Examples of eQTLs showing strong discordant effects between life stages. All eQTLs
809 are the top eQTL of the eGene in both life stages. Gene IDs and eQTL locations: a.
810 TX_paternal_00005595 (1:255437493), b. TX_paternal_00008809 (1:455264496), c.
811 TX_paternal_00013353 (2:162241243), d. TX_paternal_00014747 (2:238366426), e.
812 TX_paternal_00025461 (3:13442544), f. TX_paternal_00027513 (3:75629497).
813

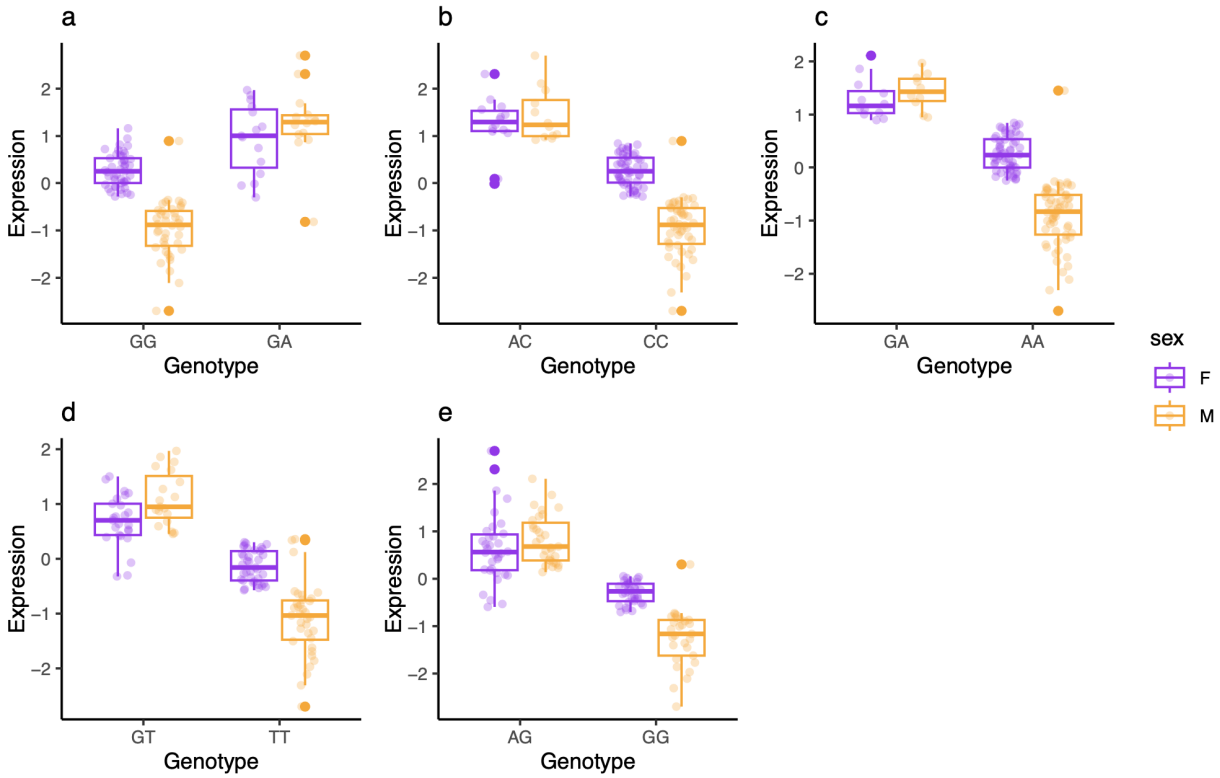

S7 Fig. Examples of eQTLs showing significant Genotype × Sex interaction in *Rumex hastatulus*. Multiple-testing corrected and Benjamini-Hochberg adjusted *p*-values: 0.00197 (a), 0.00197 (b), 0.00317 (c), 0.06472 (d), 0.07921 (e). Gene IDs and eQTL locations: a. TX_paternal_00002596 (1:159008371), b. TX_paternal_00010325 (2:14033315), c. TX_paternal_00025295 (3:10654019), d. TX_paternal_00001727 (1:70371578), e. TX_paternal_00015022 (2:250749626).

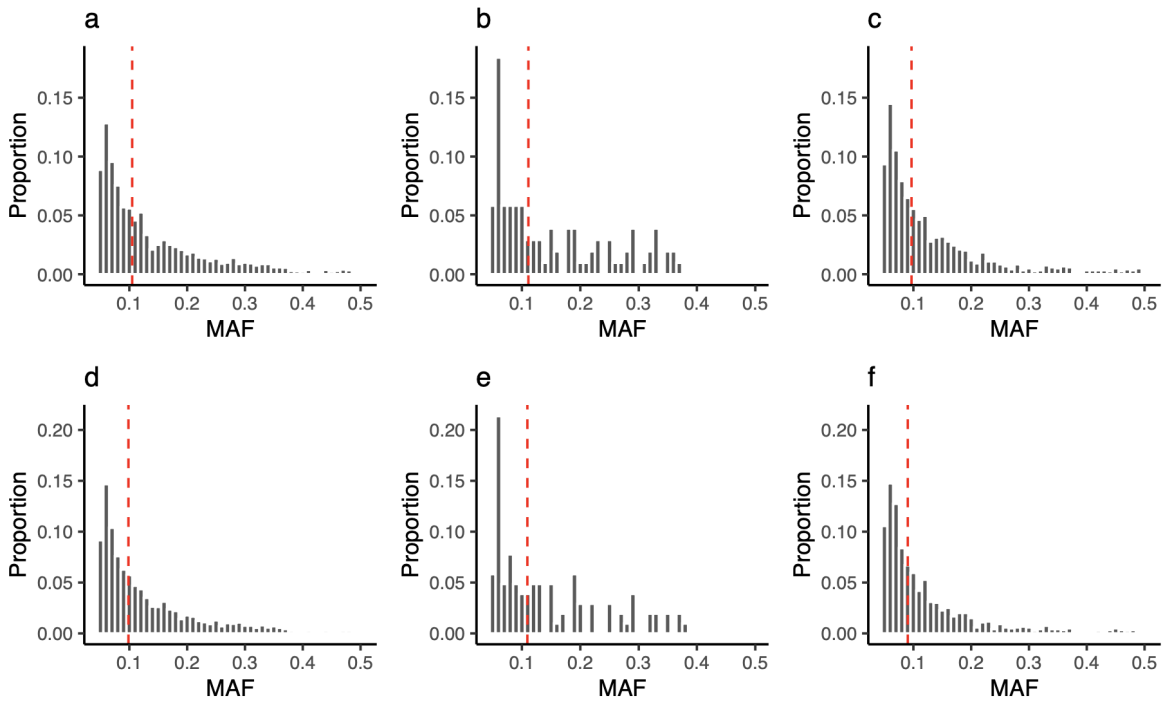

S8 Fig. The distribution of MAFs of eQTLs on autosomes (a, d), PAR (b, e) and X chromosome (c, f) in female leaf of *Rumex hastatulus*. a-c: most significant eQTLs in each eGene, d-f: randomly selected eQTLs in each eGene. Binwidth = 0.01. Median of MAFs: 0.097 (a), 0.109 (b), 0.0873 (c), 0.0938 (d), 0.107 (e), 0.083 (f).

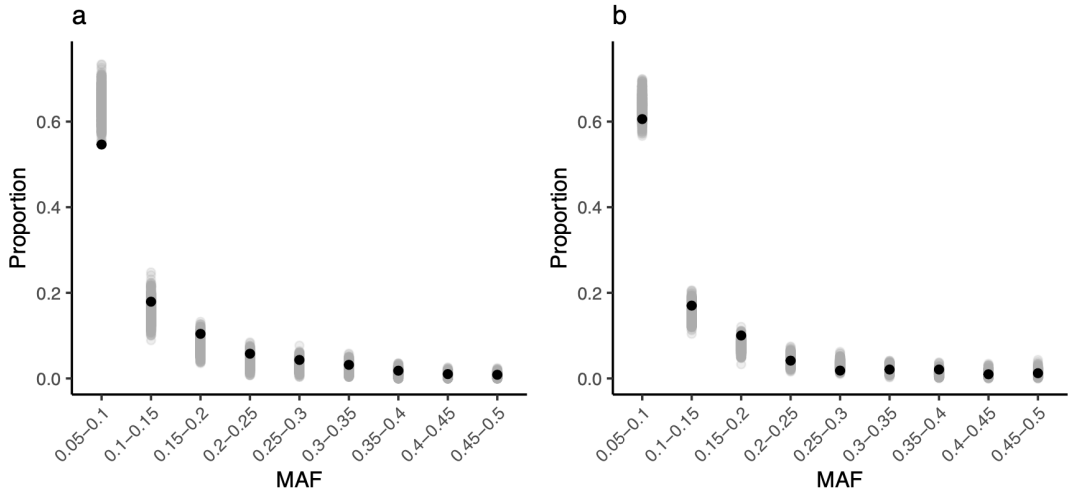

S9 Fig. Distribution of MAFs of eQTLs compared to a null distribution on autosomes (a) and X-specific regions (b) in female leaf of *Rumex hastatulus*. Black dots: true positive eQTLs (observed data), grey dots: false positive eQTLs (permuted data).